Iterative algorithm for determining optimal beam profiles in a three-dimensional space

Uriel Levy, David Mendlovic, Zeev Zalevsky, Gal Shabtay, and Emanuel Marom

A new, to our knowledge, iterative algorithm for achieving optimization of beam profiles in a three-dimensional volume is presented. The algorithm is based on examining the region of interest at discrete plane locations perpendicular to the propagation direction. At each such plane an intensity constraint is imposed within a well-defined transverse spatial region of interest, whereas the phase inside that region as well as the complex amplitude outside the region is left unchanged from the previous iteration. Once the optimal solution is found, the mask that generates the desired distribution can be readily implemented with a planar diffractive optical element such as a computer-generated hologram. Several computer simulations verified the utility of the proposed approach. © 1999 Optical Society of America
OCIS codes: 140.3300, 090.1760.

1. Introduction

The control of a beam profile along a three-dimensional (3-D) region in space is an important task in various applications such as optical scanners, displays, laser printers, and medical applications. It would be helpful to use a single diffractive optical element (DOE) to obtain any desired 3-D beam within a given volume. However, there is a major obstacle that prevents the use of a DOE in this way: The beam function must be a physical function that obeys the wave equation (or the Helmholtz equation for monochromatic illumination). For example, achieving a perfect Gaussian beam profile that remains unchanged while it propagates along the Z axis is impossible, even for a limited range, although such a beam could be helpful in a large variety of applications. Any attempt to achieve 3-D beam shaping must take this limitation into account.

A large number of approaches to achieving 3-D beam shaping have been tried during the past 20 years, including many attempts to obtain the so-called nondiffracting beams, i.e., rays that preserve their spatial properties while they are propagating along the Z axis. The trivial case of plane waves that are essentially nondiffracting beams is of no practical interest. Durnin[1] proposed an exact nondiffractive solution of the scalar wave equation: the Bessel beam. Unfortunately, this beam, which is essentially the equivalent of a collection of plane waves propagating along a conical surface, although it is interesting from a theoretical point of view, is of no practical use because it is unbounded and its generation requires an infinite amount of energy. Therefore the exact implementation of such beams is not possible. An approximate implementation of this kind of beam was achieved with DOE's.[2]

Gori *et al*. made an additional interesting attempt to achieve nondiffracting beams by defining a Gauss–Bessel beam.[3] The basic idea is to investigate the product of a Bessel beam and a Gaussian profile. Such a beam carries finite energy, and in spite of its possessing some diffraction sensitivity that is due to the Gaussian profile, its diffraction spread is less than that of an ordinary Gaussian. However, this approach is a kind of smart guess and does not promise optimal reduction of the beam spread. In addition, it does not allow arbitrary 3-D beam shaping to be achieved.

Other attempts to achieve nondiffracting beams, based on an iterative approach, were suggested by Rosen[4] and by Piestun *et al*.[5] In both of those papers it was shown that 3-D beam shaping might be achieved by use of the projection-onto-constraints sets algorithm, which is based on performing free-space propagation from one discrete plane to the next plane along the Z axis. At each plane, the function obtained is replaced by the desired constraints. The

The authors are with the Faculty of Engineering, Tel Aviv University, 69978 Tel Aviv, Israel. D. Mendlovic's e-mail address is mend@eng.tau.ac.il.

Received 26 April 1999; revised manuscript received 23 July 1999.
0003-6935/99/326732-05$15.00/0

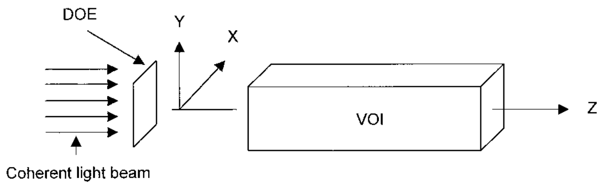

Fig. 1. Schematic of the optical setup including the volume of interest the (VOI).

replacement is then followed by propagation to the next plane. After the last plane is handled, free-space backpropagation is performed on the filter, and another iteration is initiated. The process can be stopped by any desired criterion to be defined. However, the suggested algorithm is a serial one; therefore it assigns larger weight to the far planes than to the near planes. Moreover, if the constraint in one plane is far-fetched, there is a high probability that the algorithm will not yield reasonable results.

In this paper we present a new algorithm for achieving 3-D beam shaping. Although in principle any desired shape can be implemented (with some acceptable error, as will be discussed), we have focused on the nondiffracting beam as an example that permits comparisons with other solutions. The proposed algorithm is based on a parallel rather than a serial computation; i.e., all planes are computed at one time, and the generating filter is built from averaging the backpropagation distribution from all the above data rather than by changing one plane at a time and propagating to the next one based on that change. The proposed algorithm seems to yield better results, at least for cases that have been examined, and also provides faster convergence. The output of the algorithm provides the resultant amplitude function. The above function can be implemented by use of a single phase-only filter in either an off-axis mode[6] or an on-axis mode.[7] Alternatively, the implementation of the complex amplitude function with higher efficiency in the treatment of light can be obtained with two phase-only filters separated by some propagation distance.[8,9] It should be mentioned that a method related to the proposed approach has already presented.[10] That method uses a Ping-Pong algorithm to produce 3-D displays by use of twisted nematic liquid crystals. The 3-D display task can be characterized by the small separation between discrete cross sections. Therefore the shape must change slowly between consecutive planes. In addition, high spatial resolution is needed for achieving high-quality reconstruction. Therefore we are focusing our research on 3-D beam shaping rather than 3-D displays.

The proposed approach is described in Section 2. In Section 3 we discuss the limitations of this approach. Computer simulations are finally given in Section 4.

2. Proposed Algorithm

Figure 1 illustrates the 3-D volume under consideration, in which a given light distribution should be generated. The basic assumption is that, outside that volume, no constraints exist. The proposed algorithm is based on sampling the Z axis at N perpendicular planes (cross sections) that are arbitrarily located. As a starting point for the process, we assume an initial random complex amplitude distribution, located at $Z = 0$ and represented by $u(x, y, 0)$. Free-space propagation (FSP) is then calculated from that plane to each one the N cross sections simultaneously. The FSP is achieved by use of the Huygens–Fresnel formula[11]

$$u_i(x, y, z_i) = \frac{z_i}{j\lambda} \iint \bar{u}(x', y', 0) \times \frac{\exp\{jk[z_i^2 + (x - x')^2 + (y - y')^2]^{1/2}\}}{z_i^2 + (x - x')^2 + (y - y')^2} \times \mathrm{d}x'\mathrm{d}y', \qquad i \in (1, 2, \ldots, N), \tag{1}$$

where λ is the wavelength and $k = 2\pi/\lambda$.

The next step is to apply an appropriate constraint to each cross section. Any constraint should be bounded within the predefined VOI. Outside that region, the function that is obtained is left unchanged. In addition, the phase obtained within the region should be kept unchanged as well. Mathematically, the new function at a cross section z_i can be described as

$$\bar{u}(x', y', z_i) = \begin{cases} \eta g(x', y', z_i)\exp(j\{\text{phase}[u(x', y', z_i)]\}) & (x', y') \in RO \\ u(x', y', z_i) & \text{otherwise} \end{cases}, \tag{2}$$

where $g(x', y', z_i)$ is the amplitude constraint at plane z_i and η is an efficiency coefficient that enables the energy inside the window (RO) to be controlled.

From the set of functions $u(x', y', z_i)$ one can calculate the distribution at $Z = 0$ by using free-space backpropagation from each plane Z_i:

$$u_i(x, y, 0) = \frac{-z_i}{j\lambda} \iint \bar{u}(x', y', z_i) \times \frac{\exp\{-jk[z_i^2 + (x - x')^2 + (y - y')^2]^{1/2}\}}{z_i^2 + (x - x')^2 + (y - y')^2} \times \mathrm{d}x'\mathrm{d}y'. \tag{3}$$

The filter for the next iteration can be calculated as a weighted average of the set obtained:

$$u^l(x, y, 0) = \sum_{i=1}^{N} w_i u_i(x, y, 0), \tag{4}$$

where w_i is a set of weighting coefficients and l is the iteration number. The default option is to use $w_i = 1/N$ (equal weight for each plane), although other possibilities can be chosen if some planes are more significant for the user than others.

The entire sequence above is defined as a single

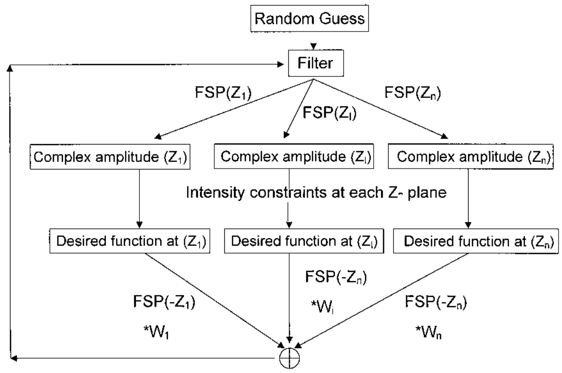

Fig. 2. Block diagram of the proposed algorithm.

iteration. One should repeat the procedure several times to achieve reasonable convergence. Possible criteria for ending the process are either completion of a limited number of iterations or arriving at some defined error metric. A block diagram of the proposed algorithm is shown in Fig. 2.

As we discussed above, it is obvious that obtaining any arbitrary desired 3-D beam shape profile is impossible unless the shape obeys the wave equation. In general, practical constraints do not fall into this category (do not obey the wave equation). However, the proposed algorithm, which is a Ping-Pong-style algorithm,[12] eventually converges toward a solution that might minimize the square error. Unfortunately, the algorithm suffers from the same drawback that is common to this family of algorithms: the minimum might be a local minimum instead of a global one. The random initial guess should be such that it will lead to achieving the global minimum. Another technique is to implant some perturbation

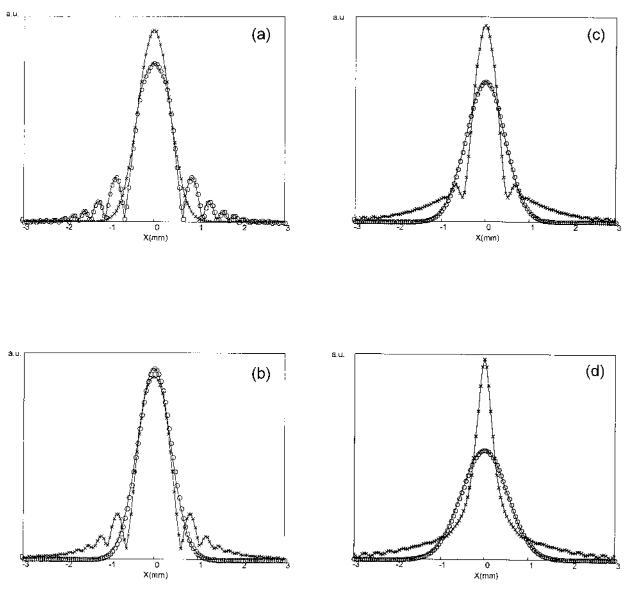

Fig. 3. Profiles at various longitudinal cross sections: crosses, the profile obtained by the algorithm; open circles, the Gaussian profile. (a) $Z = Z_0$, (b) $Z = Z_0 + 0.45$ m, (c) $Z = Z_0 + 0.9$ m, (d) $Z = Z_0 + 1.35$ m.

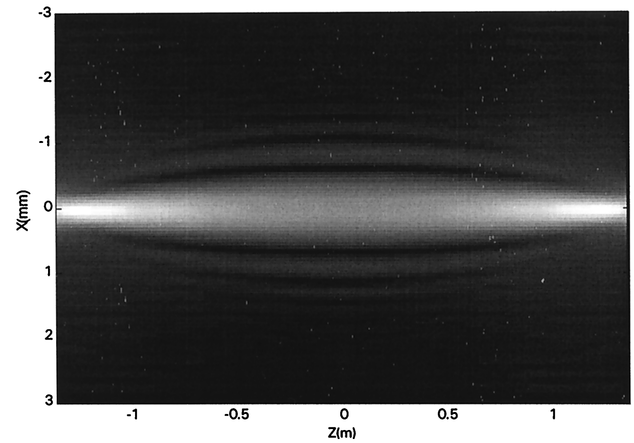

Fig. 4. Image of the profile obtained by the algorithm versus propagation distance.

within the process by means of simulated annealing. Such perturbations have the ability to get the solution out of the local-minimum well.

Another issue is that no constraints are applied for the regions between the adjacent planes, whereas one is interested in controlling the intensity distribution at all planes located inside the volume of interest. In principle, applying the above constraints at N planes does not promise the achievement of the desired intensity distribution between these planes. One simple way to overcome this obstacle is to choose a large number of planes (large N value) and thus to decrease the distances between the discrete planes. Unfortunately, such a solution requires a large computational effort and is time consuming. However, with the appropriate choice of constraints, a small N value may be sufficient. Another way to overcome this problem is to avoid using equally spaced planes. However, a better choice should be based on an approximation of a physically realizable beam with improved characteristics, for example, a modified Gaussian beam that is forced to maintain constant

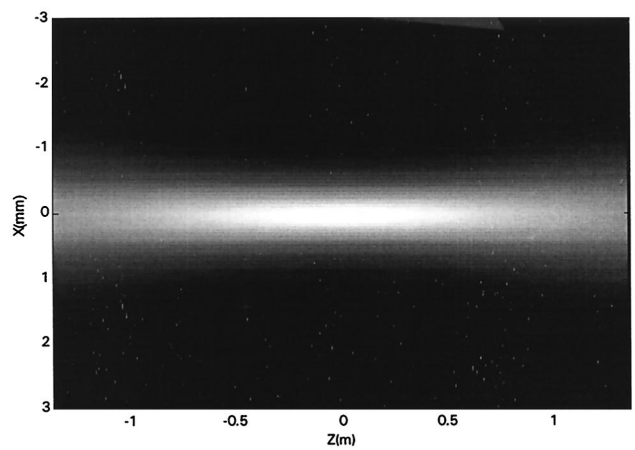

Fig. 5. Same as Fig. 4 for a conventional Gaussian beam with the same waist.

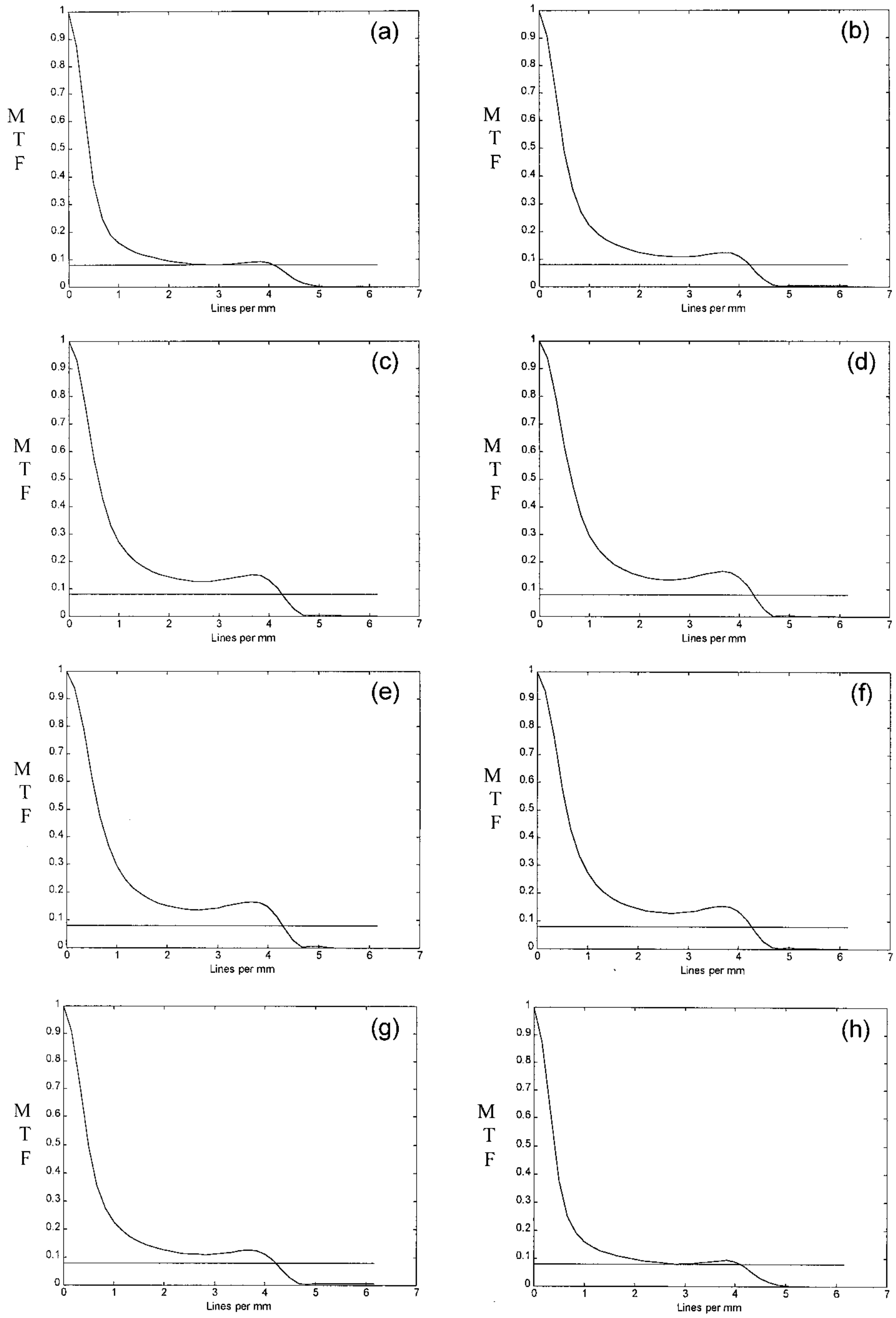

Fig. 6. MTF obtained at eight equally spaced longitudinal planes ($Z_0 - 0.4$: $Z_0 + 0.4$ m).

lateral dimensions below the conventional Gaussian beam spread, as we discuss in Section 3 below.

As a result of a comprehensive trial-and-error study, we obtained the following rule of thumb: To make the best of the proposed algorithm it is advisable to apply constraints that make use of as many degrees of freedom as possible. In practice one should make calculations based on as many pixels as possible. As a contrary example, if one will define a 3-D beam-shaping task of achieving a delta function surrounded by a large region of zero energy, no degrees of freedom will be left, and a poor solution will be obtained. Hence to increase the relative number of degrees of freedom one should avoid increasing the VOI size more than necessary.

3. Computer Simulations

To demonstrate the capabilities of the proposed approach, we performed some computer simulations. The first set of simulations was based on a Gaussian profile. As a constraint we used a Gaussian beam with a waist of 0.5 mm (located at $Z_0 = 1.65$ m) and required that the beam spread 80% less than an ordinary Gaussian beam. We applied this constraint to 11 planes. The distance between two adjacent planes was 27.5 cm, the total propagation distance was 2.7 m ($Z_0 \pm 1.35$ m), and $\lambda = 0.632$ μm. We used only 50 iterations to emphasize the fast convergence rate. In Fig. 3 the cross sections of the beam that we obtained are displayed at four different planes ($Z = Z_0, Z = Z_0 + 0.45$ m, $Z = Z_0 + 0.9$ m, and $Z = Z_0 + 1.35$ m). For comparison, cross sections of a conventional Gaussian beam with the same waist at $Z = Z_0$ are also presented. The beam behaves symmetrically for $Z_0 - 1.35 < Z < Z_0$. Figure 4 is an image of the beam's lateral profile relative to the propagation distance (Z). Figure 5 is the same image for a conventional Gaussian beam with the same waist at $Z = Z_0$. From these figures one can see that a higher confinement of the beam has been achieved by the proposed approach. The waist is approximately one half of the Gaussian waist at the VOI edge ($Z = 1.35$ m). Note that the task has been achieved in the whole 3-D VOI (not only in the discrete planes). The DOE dimensions are 6×6 mm. 256×256 pixels were used; therefore the feature size is ~23.5 μm. We ignored the phase quantization, assuming that with current technologies (as many as 32 phase levels) the quantization effect is negligible.

As an attempt to confront a practical aspect of the problem we carried out another set of computer simulations. The task now is to form a beam that, when it is used for scanning, provides a modulation transfer function (MTF) response that is higher than 8% for frequencies of as many as 4.1 line pairs per millimeter within the VOI. These properties should be maintained for a propagation distance of 0.8 m. The MTF is calculated as the Fourier transform (FT; along the X direction) of the line-spread function. Thus it is given by

$$\mathrm{MTF}[u(x, y)] = \frac{\left| \mathrm{FT}\left[\int_{-\infty}^{\infty} |u(x, y)|^2 \mathrm{d}y \right] \right|}{\left| \mathrm{FT}\left[\int_{-\infty}^{\infty} |u(0, y)|^2 \mathrm{d}y \right] \right|}, \quad (5)$$

As an initial guess we chose the optimal Gauss–Bessel beam (according to Ref. 9 for this task:

$$|u(r)| = \left| \exp\left[-\left(\frac{r}{w} \right)^2 \right] J_0\left(\frac{2\pi}{\lambda} ar \right) \right|, \quad (6)$$

where $w = 0.95$ mm, $a = 1.32\,e - 3$, and $\lambda = 0.632$ μm. The MTF's at several planes can be seen in Fig. 6. As expected, the best MTF response was obtained in the middle of the region, and some degradation can be observed toward the edges. Nevertheless, the task of tight confinement with limited spread has been achieved. For comparison, the ordinary Gauss–Bessel beam possesses 10% less working range for the same MTF parameters. The addition of the Bessel beam in Eq. (6) provides an effective waist of the Gauss–Bessel beam of only 0.133 mm. We estimated this value by assigning the Bessel argument a value of 1.75. For this value, the Bessel function falls to $1/e$ of its maximal value. For such a waist value the Gaussian beam's active range (assuming the same MTF parameters) is only 0.15 m. As before, we used 6 mm $\times$ 6 mm DOE with 256×256 pixels; therefore a feature size of 23.5 μm has been assumed. Again, phase quantization was ignored.

4. Conclusions

A novel algorithm for achieving three-dimensional beam formation within a predefined volume of interest (VOI) has been proposed. The algorithm is an iterative one and is based on dividing the 3-D space into discrete planes (cross sections) that are perpendicular to the direction of propagation. At each cross section an intensity constraint is imposed inside the VOI and the phase inside that volume, as well as the complex amplitude outside the volume, is left unchanged from the value obtained in the previous iteration. This approach can be implemented with a diffractive optical element (DOE) such as a computer-generated hologram (CGH).

Several cases related to the generation of confined beam have been studied and demonstrated by computer simulations. The results indicate that improved 3-D beam shaping can be achieved by this approach and that practical problems can be treated.

U. Levy and G. Shabtay acknowledge financial support from the Israeli Ministry of Science and the Arts.

References

1. J. Durnin, "Exact solutions of nondiffracting beams," J. Opt. Soc. Am. A **4,** 651–654 (1987).
2. A. Vasara, J. Turunen, and A. T. Friberg, "Realization of general nondiffracting beams with computer-generated holograms," J. Opt. Soc. Am. A **6,** 1748–1754 (1989).
3. F. Gori, G. Guattari, and C. Padovani, "Bessel–Gauss beams," Opt. Commun. **64,** 491–495 (1987).
4. J. Rosen, "Synthesis of nondiffracting beams in free space," Opt. Lett. **19,** 369–371 (1994).
5. R. Piestun, B. Spektor, and J. Shamir, "Wave fields in three dimensions: analysis and synthesis," J. Opt. Soc. Am. A **13,** 1837–1848 (1996).
6. A. W. Lohmann and D. P. Paris, "Binary Fraunhofer holograms, generated by computer," Appl. Opt. **6,** 1739–1749 (1967).
7. D. Mendlovic, G. Shabtay, U. Levy, Z. Zalevsky, and E. Marom, "Encoding techniques for the design of zero-order (on–axis) Fraunhofer computer-generated holograms," Appl. Opt. **36,** 8427–8434 (1997).
8. D. Mendlovic, Z. Zalevsky, G. Shabtay, and E. Marom, "High-efficiency arbitrary array generator," Appl. Opt. **35,** 6875–6880 (1996).
9. E. Marom, D. Mendlovic, N. Konforti, J. Katz, and C. Tan, "Diffractive optic elements for forming scanning beams," in *Diffractive and Holographic Device Technologies and Applications IV*, I. Cindrich and S. H. Lee, eds., Proc. SPIE **3010,** 30–37 (1997).
10. T. Haist, M. Schönleber, and H. J. Tiziani, "Computer-generated holograms from 3D objects written on twisted-nematic liquid crystal displays," Opt. Commun. **140,** 299–308 (1997).
11. J. W. Goodman, *Introduction to Fourier Optics* (McGraw-Hill, New York, 1996), p. 66.
12. R. W. Gerchberg and W. O. Saxton, "A practical algorithm for the determining of phase from image and diffraction plane figures," Optik **35,** 237–246 (1972).